A Critical Review of Fatigue Life Prediction on 316LN SS

Raj Kumar, Mohammad Mursaleen, G. A. Harmain, and Ashutosh Kumar

Abstract Fatigue failure is referred to the slow deterioration process of structures that are subjected to cyclic loading, including the structural elements of nuclear power plants, aircraft, railways, and rotating machinery. During their operating life, high-temperature components resist three major damaging phenomena: creep, fatigue, creep-fatigue interaction (CFI), and oxidation. Temperatures, strain amplitude, strain rates, hold period effect on fatigue, creep-fatigue interaction, and fatigue crack growth (FCG) for 316LN stainless steel (SS) are presented, and dynamic strain aging (DSA) role is discussed in the article. The fatigue life (FL) increases with nitrogen content (NC), and reduction in the stress precipitation and stress relaxation (SR) due to changes in dislocation structure are given in detail. Fatigue life decrease with increasing hold time is also presented.

Keywords 316LN Stainless steel · FCG · Low-cycle fatigue · DSA

1 Introduction

316LN stainless steel is selected for its high-temperature (HT) service conditions as it shows good weldability, intergranular stress corrosion and chloride-induced crack, adaptability with sodium coolants, and corrosive environments [2, 3, 67, 75]**.** It has been extensively used in nuclear power plants, thermal power plants, and aircraft components that operate at elevated temperature [33, 43, 73]. High nitrogen content (0.22%) enhances elevated temperature creep resistance, fatigue, and fracture strength [13, 31, 60]. During thermomechanical processes, 316LN SS experiences several metallurgical changes including flow instabilities, work hardening, dynamic recovery, and dynamic recrystallization [51]**.** Dynamic recrystallization nucleation produces in subgrain growth and grain boundary projecting mechanism [71]. Mechanical strength of 316LN SS decreases with increasing temperature. The

R. Kumar · M. Mursaleen (✉) · G. A. Harmain · A. Kumar
Mechanical Engineering Department, National Institute of Technology Srinagar, Srinagar, J&K 190006, India
e-mail: mursaleen@nitsri.net

R. P. Singh et al. (eds.), *Advances in Modelling and Optimization of Manufacturing and Industrial Systems*, Lecture Notes in Mechanical Engineering,
https://doi.org/10.1007/978-981-19-6107-6_30

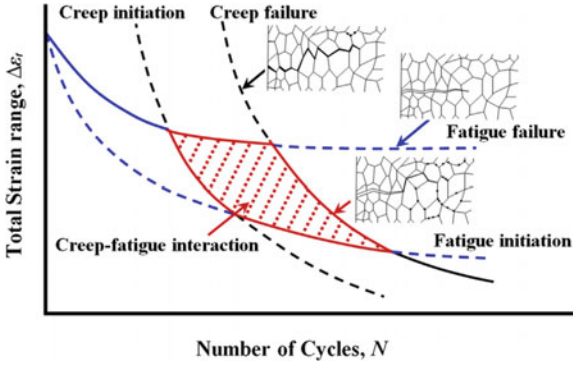

Fig. 1 Schematic diagram of CFI and failure modes due to fatigue and CFI [73]

strain-induced martensite increases the fracture stress during the impact test [72]**.** Under high-temperature start–stop conditions, temperature and load vary with time, resulting in a combination of creep and fatigue deformation [29, 32, 37, 61]. Due to cavitation damage, creep damage can occur during the holding period and is usually manifested as a creep cavity at the grain inner edge [74]. While in creep-fatigue interactions, strong cavitation damage is observed in this material, and fatigue crack damage develops on the surface. When this interaction occurs, the failure mode is mixed (transgranular as well as intergranular), as shown in Fig. 1 [16, 48]. Elastic–plastic fracture mechanics (EPFM) is a tool for determining the leak before break (LBB) of pressurized piping systems and estimating the service life of reactor vessels [30].

2 Research Background

Structural components which are subjected to cyclic loading such as elements of nuclear power plants, aircraft, and rotating machinery, fatigue life assessment study were presented by [23]. There are three stages: initiation of cracks, development of short crack to long crack, and ultimately fracture of the component [68]. The Paris rule is generally accepted as a useful method for measuring fatigue crack extension rate with a stress intensity factor [20, 63]. Modeling and simulating the fatigue crack extension mechanism of various structural components is of utmost importance to ensure safety and reliability under different loading conditions [17, 21]. An enormous number of numerical techniques have evolved to simulate the crack extension problem [26, 27] and fatigue [24] like as the finite element method (FEM), boundary element method (BEM), and an extended finite element method (XFEM) [13]. XFEM is an effective numerical technique for simulating various discontinuities, such as cracks, contact [34, 36] inclusions [35], and cavity without the need for a finite element mesh to correspond to these discontinuities [13, 25].

Samuel et al. [52], studied the tensile work hardening behavior of 316LN SS at different temperatures and strain rates. It has been observed that the tensile properties of the material are changed at intermediate temperatures due to dynamic stress aging. Experimental results show that the load-deformation curves were smooth at ambient and HT, whereas at a medium temperature, the irregular flow was obtained. Srinivasan et al. [66], investigated the LCF and CFI behavior of 316LN SS under different experimental condition such as various deformation behavior on this material reported based on several mechanisms including DSA under stress, creep, oxidation, and sub-structural recovery. Using the data generated in that study, an artificial neural network (ANN) model enabled life prediction model under LCF and CFI conditions.

Kim et al. [28], conducted LCF and CF tests for two materials (316L and 316LN SS) with continuous cycling and 10-min hold period at temperature 600 K in air. It was noticed that the addition of nitrogen increased FL, CF life, and saturation stress. It is reported that the fracture mode in the fatigue test was transgranular and for the CF test was intergranular. In addition, the dislocation structure for 316L was cellular and planar for 316LN in the fatigue, creep-fatigue test. Precipitation of carbides at grain boundaries has been reported in CF tests, and it has been suggested that these precipitation can be avoided with addition of nitrogen. Roy et al. [49] examined the LCF tests of 316LN SS at room temperature with the range of strain amplitude ($\pm$ 0.3 to $\pm$ 1.0%) and strain rate ($3 \times 10^{-3}s^{-1}$). The material exhibited non-masing behavior at higher strain rates and masing behavior at lower strain rates. It has been reported that FL decreases with increasing stress amplitude, and the hysteresis loop behavior was in good agreement with the test results. Babu et al. [3], conducted FCG test on 316LN SS at room temperature; the nitrogen percentage was varied through 0.8, 0.14, and 0.22 wt%. In this study, the direct current potential drop (DCPD) technique was used to estimate FCG, and the compliance technique was used to estimate the crack closure. It was observed that the threshold stress intensity factor (ΔKth) and effective threshold stress intensity factor $\Delta K_{\text{eff.}}$th were different for various nitrogen contents. Also, the fracture surface roughness parameter was used to quantify the slip irreversibility model. The cracks are often formed by the microcavity nucleating, growing, and converging, as shown in Fig. 2 [75].

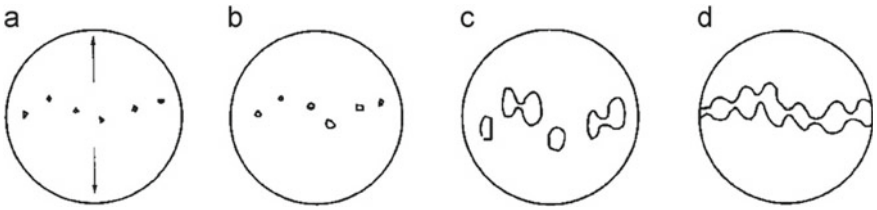

Fig. 2 Crack formation involves **a** cavity nucleation, **b** cavity growth, **c** cavity polymerization, and **d** fracture [75]

3 Factors Affecting Mechanical Properties of 316LN SS

The effect of temperature and strain rate, hold period, nitrogen content, and dynamic strain aging on deformation behavior of 316LN SS has been discussed in this study.

3.1 Effect of Temperature and Strain Rate

The load-deformation curve is smooth at room and elevated temperature although irregular flow curves were obtained at intermediate temperatures**.** The sufficient plastic stress–strain data for 316LN SS are best expressed in terms of Ludwigson relation at ambient temperature [8, 72]. Several flow parameters observed in the Ludwigson–Voce equation varies with deformation rate and temperature [8]. The decrease in FL with an increase in the temperature range (673–873 K) is ascribed to detrimental effects of DSA, and beyond 873 K, the FL was affected by oxidation [56, 64]. This material exhibited a higher ratio of normalized stress with increasing temperature (573–873 K) and also observed irregular fluctuation in tensile properties due to DSA at a medium temperature and a normal behavior at elevated temperatures [66]. Isothermal cycling at the HT of thermomechanical fatigue yielded lower endurance than in-phase and out-of-phase cycling [44]. The ratcheting strain increases with an increase in temperature, and fatigue life decreased because of higher plastic deformation [58].

In the load-deformation curve, irregular flow/twitching at the mean temperature is observed, related to the attractive interaction between the solute and the mobile dislocation throughout deformation, known as DSA [45, 52, 56]. DSA temperature regime is sensitive to nitrogen percentage, with temperatures ranging from 673 to 873 K (Fig. 3a) for nitrogen percentage less than 0.11 wt% and from 773 to 873 K (Fig. 3b) for nitrogen percentage greater than 0.11 wt% [45]. The direction of generating a set of non-cellular displacements increased with increasing DSA. 316LN SS is available in two irregular flow temperature regimes, such as the relatively low temperature (523–598 K) and the high temperature (673–923 K) [8].

A low-cycle fatigue test was conducted for short cycles, and no evidence of dynamic precipitation in the temperature range associated with rapid cycle hardening. That study explicitly ruled out a precipitation effect in the rapid hardening of 316LN SS**.** The fatigue strength decreased by increasing the temperature and decreasing the strain rate from 3×10^{-2} to $3 \times 10^{-5} s^{-1}$ [66]. At all strain rates of 773 and 823 K, DSA played a vital role in fatigue deformation and fracture. In tensile tests at 873 K, DSA has been reported to result in a decrease in service life and increased fatigue strength. DSA has been described to cause hardening at an earlier fatigue life stage, and nitrogen retarded influence of DSA [28]. Samantaray et al. [50] This article has reported the influence of strain rate, deformation, working environment (temperature), and method of loading on tensile behavior of 316LN,

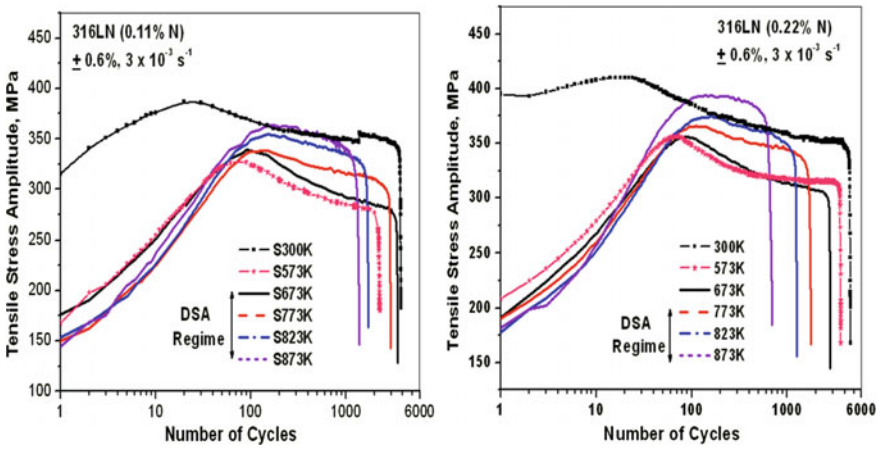

Fig. 3 Cyclic stress response (CSR) curves of 316LN SS alloyed with different nitrogen contents [45]

and a correlation between deformation and microstructural features has been established. The higher temperature regime of 316LN SS serrated flow conflicts with the temperature range (773–973 K) in which precipitation of chromium carbide has been observed. In the low-temperature range (523–623 K), the diffusion of interstitial solutes to displacements is responsible for serrated flow. The mechanism accountable for the serrated yielding in the HT range (973–923 K) is an alternative solute like Cr [54].

3.2 Effect of Hold Period

The SR behavior in the cyclic regime at half-life was presented by the CFI, which introduced hold time at the peak tensile strain or peak compression strain as shown in Fig. 4 [73].

CFI tests have been conducted at 873 K to estimate the impact of the hold period (1–90 min). It has been reported that there was a reduction in fatigue resistance with an increase in hold time**.** CFI is caused by a flaw in the grain boundary that leads to creep in the intergranular cavity, which can lead to intergranular gaps and cracks that coincide with fatigue cracking and constitute the most common cause of premature failure [66]**.** It has been found that SR varies with nitrogen content and saturating stress during the hold time [6, 40]. In CF experiments, the creep deformation occurring during the hold period has been evaluated to play a vital role in nucleation and growth of voids indicating the occurrence of an intergranular failure mode attributed to gap nucleation at the grain boundary [28].

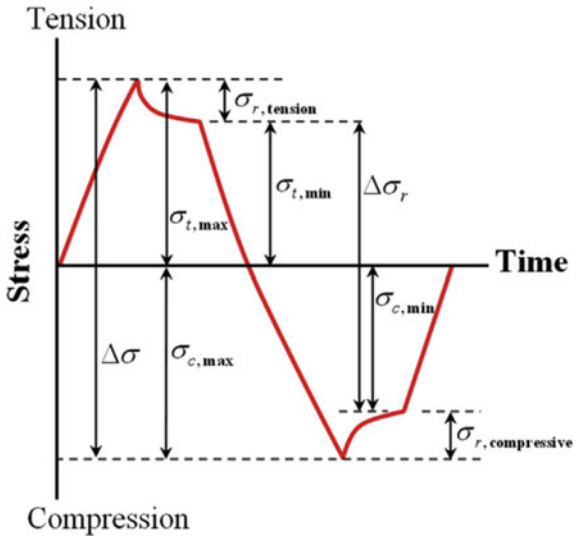

Fig. 4 In hold-time tests, different stress values were found [73]

The occurrence of creep during hold time results in the reduction of cyclic stress to attain a given strain in creep-fatigue tests [61]. Declaring that 316LN stainless steel has a high DSA in the temperature range (573–923 K), cyclic hardening behavior develops. However, the planar dislocation structure deteriorates, and the dislocation density decreases during the hold time; the resistance to dislocation motion decreases [10, 28]. In CF tests, at a constant temperature and plastic strain range, FL is found to be reduced, while the tensile hold time is increased [39]. Sarkar et al. [57], Conducted creep-fatigue interaction experiment at elevated temperature (650 ˚C) for 316LN SS where selected loading parameter is below endurance strength with high load ratio. They reported that small load amplitude shows substantial CFI which indicates the influence of stress amplitude on the failure mechanism of material at higher temperatures.

3.3 Effect of Nitrogen Content and Dynamic Strain Aging

Nitrogen has been reported to affect fatigue and creep properties at HT by modifying metallurgical factors like dislocation, precipitation, and DSA. With the addition of nitrogen percentage, the dislocation structure is changed from unitary to planar in the fatigue and CF tests [40]. The temperature and time for carbide precipitation have been reported to increase by the addition of nitrogen [41]. The integrated effect of precipitation strengthening by excellent carbides and substantial solution strengthening by nitrogen in 316LN SS resulted in increased creep rupture life and decreased creep life [38]. High-temperature LCF life increased with the adding nitrogen because it produced planar slip and restrained DSA [28, 29, 43, 65].

The fatigue strength at 300 and 77 K increases with the addition of nitrogen [70]. The creep and tensile endurance of 316LN SS was reported to improve significantly by enhancing the nitrogen percentage [37, 44] and also improving fracture toughness at cryogenic temperatures [31]. Surface and internal creep damage decreased with an increase in nitrogen percentage [13]. The steady-state creep rate, the region of intragranular cracks, and surface cracks reduced with an increase in nitrogen percentage [62]. The addition of nitrogen to 316LN SS improved corrosion resistance by preventing pitting, intergranular corrosion, sensitization, corrosion fatigue, and stress corrosion cracking [18]. Two typical manifestations of dynamic strain aging have elastic shakedown and strain burst [55]. The cyclic stress response of 316LN steel is observed to show initial hardening, softening, saturation, and eventual fracture over a long period [45, 49]. Addition nitrogen in austenitic stainless steels (304LN and 316LN SS) shows a beneficial effect on flow strength via strain hardening characteristics which can be attributed to bulk material strengthening and inclination toward planar slip hence, trim downs the susceptibility to dynamic recovery [42].

The effect of nitrogen on the CSR was observed in the LCF test with a strain amplitude of 0.6% and an ambient temperature of 300 K. The degree of softening increased by increasing the nitrogen percentage, especially for 0.14 and 0.22% at 300 K [47]. The CSR with a strain amplitude of $\pm$ 0.6% develops into a plastic deformation greater than the strain amplitude of $\pm$ 0.4% [59]. The CSR increased with decreasing strain rate as depicted in Fig. 5 which shows variation of half-life tensile stress amplitude (HLSA) with respect to nitrogen percentage at different strain rates of $3 \times 10^{-5} s^{-1}$and$3 \times 10^{-4} s^{-1}$ and temperatures [43]. The CSR of 316LN SS under high-temperature fatigue loading is influenced by multiple factors such as dislocation–dislocation and interaction, DSA, recovery process, and creep [12, 32]. Dynamic strain aging (DSA) is based on time and temperature phenomena**.** When DSA reduces ductility, it may affect crack propagation at high temperatures, as seen in Fig. 6 [29]. The activation energy of 200 kJ mol^{-1} was attained in temperature range (673–873 K), which encourages the opinion that the diffusion of exchange elements such as Cr to dislocation was produced by the DSA [65]. In LCF experiments, it is also significant that nitrogen percentage greater than 0.07 wt% results in substantially larger cyclic tensile stresses [29]. Ganesan et al. [11], studied the deformation behavior of 316LN SS at high temperature and constant load (creep) for varying nitrogen percentage at 650 ˚C and reported that material creep resistance increases with increasing nitrogen percentage (0.07–0.22%) while creep ductility decreases. Increasing nitrogen percentage increases the tendency of intergranular deformation, while in the case of low nitrogen it shows both transgranular as well as intergranular cracking. Fatigue crack propagation at elevated temperature is governed by intergranular mode, due to the synergetic effect of DSA and oxidation, while in absence of oxidation, fatigue damage will transgranular [76].

The influence of nitrogen percentage in 316LN on LCF life can be obtained only when the time-dependent effects are minimum and the failure mode is typically transgranular, as shown in Fig. 7, [43].

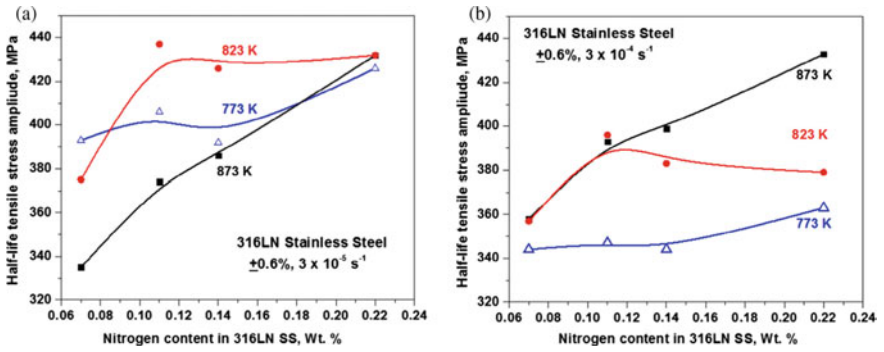

Fig. 5 Effect of temperature on 316 LN with two strain rates and variation in nitrogen content [43]

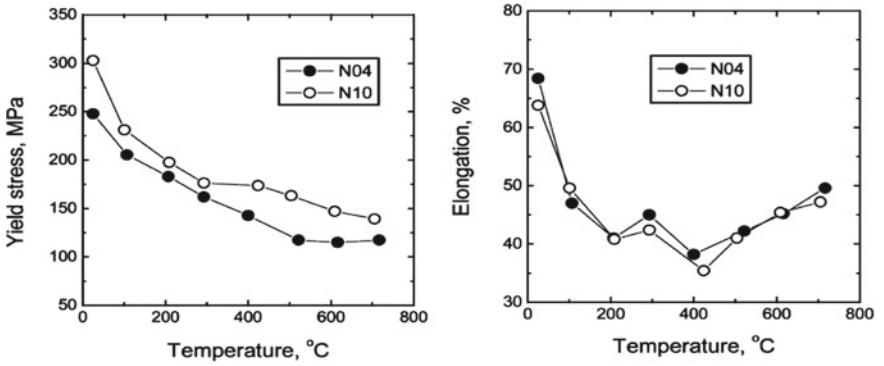

Fig. 6 Effect of temperatures on yield stress and elongation for 316LN SS [29]

The flow stress rises with reducing deformation rate but increases with increasing temperature [46, 65]. It was observed that for 0.14% N steel, the strain increased by 0.4% with increasing temperature (773–873 K), and the strain amplitude was 0.6%, showing DSA. The initial cyclic hardening of 773 and 300 K, with a deformation magnitude of 0.6%, occurred during DSA. In the stress–strain hysteresis loop, 0.07 and 0.22% N of the steel at all stress amplitudes of 873 and 823 K were irregular flow, independent of the nitrogen. A continuous cyclic decrease in the degree of stress drop associated with tensile results was observed over the half-life period [46]. The influence of nitrogen on FL was observed at 773 and 873 K with strain amplitudes between 0.25 and 1.0%. It was also observed that the fatigue life increases or decreases with changing nitrogen content or becomes saturated with temperature and amplitude of applied strain at 0.14% N [47]. Reddy et al. [47], conducted LCF tests with a strain amplitude of 0.25% and at temperatures 773 and 873 K. It has been reported that the cyclic strain is influenced by DSA and secondary cyclic hardening (SCH) for 0.14% N steel. DSA is exhibited as a general increase in stress response with increasing temperature except at 873 K, whereas SCH is observed throughout

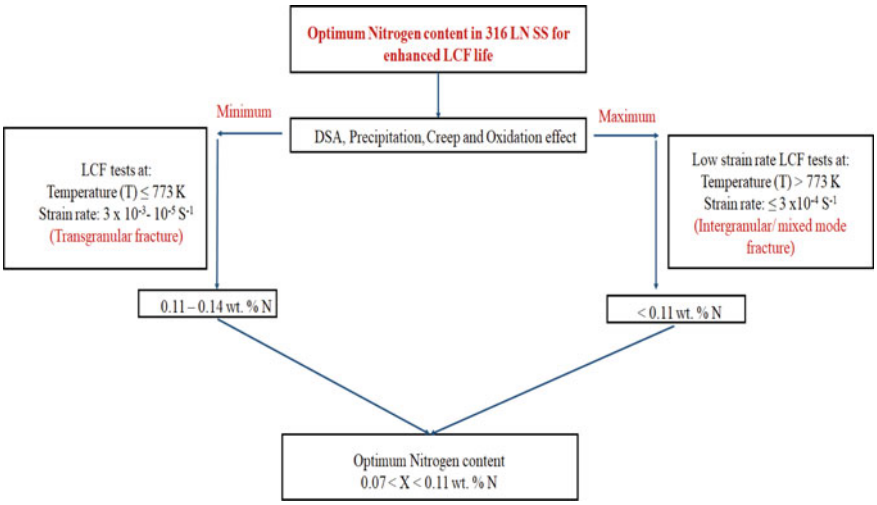

Fig. 7 Increased LCF life for 316LN SS with optimum nitrogen percentage is due to time-dependent processes

the full temperature range from 773 K to 873 K with different amounts of hardening (during SCH) at each temperature. During SCH, increasing the nitrogen content and decreasing the temperature can increase the degree of hardening. At 773 K, DSA and SCH develop matrix hardening, and the life of LCF falls with increasing nitrogen content due to the rapid propagation of cracks during matrix.

Hardening [45, 47]. In LCF tests with a strain amplitude of ± 0.4% and a temperature of 873 K, 316LN SS displayed constant CSR from the initial cycle until it reached a near-saturated state before a rapid decrease in stress (GV and GA 2018). In the high-temperature regime, deformation rates of the load-deformation curves and temperature-dependent fragmentation flow dissipation occur. [69] In a research paper, the effect of sub-creep temperature on dynamic strain aging which influence the hardening behavior was analyzed. 316LN SS, DSA exists between 523 and 923 K; the material tends to have minimal ductility, and it has been observed that fracture resistance diminishes with rising temperature [9].

3.4 Effect of Temperature on Fatigue Crack Growth

The FCG experiments were conducted at temperatures from 300, 573, and 823 K in the air using the ΔK decreasing mode under a constant R of 0.1 at a loading frequency of 15 Hz as shown in Fig. 8. The online crack length was estimated with the help of the direct current potential drop (DCPD) method [4]. The 0.22% N steel exhibited a larger FCG rate and lower threshold stress intensity factor (ΔKth) in the Paris regime than the 0.14% N steel. The FCG results with crack closure correction,

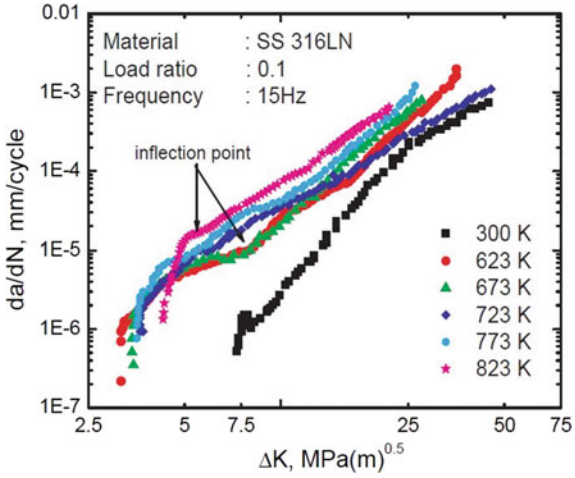

Fig. 8 Effect of various temperatures on the FCG behavior of SS316LN [4]

FCG resistance of 0.14% N steel is better than the other two 0.08 and 0.22% N steel in Paris and threshold regimes [3, 60]. Nitrogen is useful to the LCF resistance while the high slip planarity and decrease in stacking fault energy (SFE), which produces a high tendency to slip reversibility and reduces the cyclic strain localization [32, 44]. The 316LN SS will damage by creating stacking fault rings during the comparable stress that leads to a significant level of nearly 600 MPa due to several encouraging measures including radiance, raising strain, and diminishing test temperature [7]. A complex microstructural phenomenon governs the initiation of intragranular cracks during the LCF test [62]. Plastic deformation induces an effect on fatigue crack propagation was reported in [19].

While in the case of various loading patterns, loading patterns are associated with crack tip stress–strain behavior which controls the fatigue crack propagation rate [22]. The anisotropic behavior of SS 316LN at this microscopic level has been shown to perform an essential role in the development of fatigue cracks**.** Fatigue cracking depends on 316LN stainless steel's graininess for surface cracks without damages and existing cracks [9, 63]. (Zhang et al. [76]) found that the environmental-aided effect on FCG rate was equivalent to the K value and that under the same K and rise time situations, the increase in FCG rate in HT water became more evident as the load ratio (R) value raised. The influence of grain boundary atmosphere distribution and grain size on corrosion fatigue analysis of 316LN SS in borated and lithiated HT water was examined by [14]. The grain boundary engineering method, rather than increasing the fraction of low-coincidence site lattice boundaries, was found to improve FL due to grain refining. The 316LN SS undergoes significant hardening under both cold and hot conditions. The plastic deformation of 316LN SS was formulated and depends on various processing parameters like deformation amplitude, deformation rate, temperature, and load type [50]. Samuel et al. [53], In this article, effect of varying load ratios on fatigue crack threshold has been reported and found that threshold stress intensity factor has an inverse relation with load ratio. The hardness

value of 316LN stainless steel increases with increasing deformation rate, reaching a maximum amount of 350 HV at a maximum applied deformation rate of $3 \times 10^{-3} s^{-1}$ [1]. The growth rate of fatigue cracking decreases with an increasing load angle. Using different ranges of stress intensity factors, FCG rate da/dn of mode-I is lower than that of the mixed mode [5].

4 Conclusion

The interaction between creep-fatigue and fatigue has been studied in this review. In the secondary cyclic hardening process, hardening is increased by increasing the nitrogen content and with the decrease in temperature. Dynamic strain aging is a time and temperature-dependent phenomenon, so yield strength increases with decreasing deformation rate or increasing temperature. Adding nitrogen increases the life of the high-temperature low-cycle fatigue as it creates glide and preserves dynamic strain aging. With increased hold duration, fatigue life decreases.

References

1. Acharya S et al (2019) Effect of high strain rate deformation on the properties of SS304L and SS316LN Alloys. Mech Mater 136:103073
2. Babu MN et al (2010) On the anomalous temperature dependency of fatigue crack growth of SS 316(N) weld. Mater Sci Eng A 527(20):5122–5129
3. Babu MN et al. (2013) Fatigue crack growth behavior of 316LN stainless steel with different nitrogen contents. Proc Eng 55:716–21
4. Babu MN, Sasikala G (2020) Effect of temperature on the fatigue crack growth behaviour of SS316L (N). Int J Fatigue 140:105815
5. Babu MN, Venugopal S, Sasikala G (2014) Evaluation of fatigue crack growth behaviour of SS 316 LN steel under mixed mode loading (Mode I and II). Proc Eng 86:639–644
6. Brinkman CR (1985) High-temperature time-dependent fatigue behaviour of several engineering structural alloys. Int Met Rev 30(1):235–258
7. Byun TS, Lee EH, Hunn JD (2003) Plastic deformation in 316LN stainless steel-characterization of deformation microstructures. J Nucl Mater 321(1):29–39
8. Choudhary BK, Isaac Samuel E, Bhanu Sankara Rao K, Mannan SL (2001) Tensile stress-strain and work hardening behaviour of 316ln austenitic stainless steel. Mater Sci Technol 17(2):223–231
9. Dutt BS et al (2014) Effect of nitrogen addition and test temperatures on elastic-plastic fracture toughness of SS 316 LN. Proc Eng 86:302–307
10. Fan Y-N, Shi H-J, Tokuda K (2015) A generalized hysteresis energy method for fatigue and creep-fatigue life prediction of 316L (N). Mater Sci Eng A 625:205–212
11. Ganesan V et al. (2022) Role of nitrogen content on interrelationship between creep deformation and damage behaviour of 316LN SS. Trans Indian National Acad Eng 1–9
12. Ganesan V, Mathew MD, Parameswaran P, Laha K (2013) Effect of nitrogen on evolution of dislocation substructure in 316LN SS during creep. Proc Eng 55:36–40
13. Ganesan V, Mathew MD, Parameswaran P, Bhanu Sankara K, Rao. (2010) Creep strengthening of low carbon grade type 316LN stainless steel by nitrogen. Trans Indian Inst Met 63(2):417–421

14. Gao J, Tan J, Wu X, Xia S (2019) Effect of grain boundary engineering on corrosion fatigue behavior of 316LN stainless steel in borated and lithiated high-temperature water. Corros Sci. https://doi.org/10.1016/j.corsci.2019.01.036
15. GV, Prasad Reddy, and Harmain GA. (2018) Simulation of low cycle fatigue stress-strain response in 316LN stainless steel using non-linear isotropic kinematic hardening model—a comparison of different approaches. Fatigue Fract Eng Mater Struct 41(2):336–347
16. Hales R (1980) A quantitative metallographic assessment of structural degradation of type 316 stainless steel during creep-fatigue. Fatigue Fract Eng Mater Struct 3(4):339–356
17. Jameel A, Harmain GA (2016) Modeling and numerical simulation of fatigue crack growth in cracked specimens containing material discontinuities. Strength Mater 48(2):294–307
18. Jayakumar T et al (2013) Nitrogen enhanced 316LN austenitic stainless steel for sodium cooled fast reactors. Trans Tech Publ, In Advanced Materials Research, pp 670–680
19. Kant C, Harmain GA (2021a) An investigation of constant amplitude loaded fatigue crack propagation of virgin and pre-strained aluminium alloy. In: International conference on advanced manufacturing and materials processing (CAMMP 2021), Bentham Science Publishers, Jaipur
20. Kant C, Harmain GA (2021b) An investigation of fatigue crack closure on 304LSS and 7020-T7 aluminium alloy. In: International conference on progressive research in industrial and mechanical engineering (PRIME-2021), Patna
21. Kant C, Harmain GA (2021c) Fatigue life prediction under interspered overload in constant amplitude. In: 9th International conference on fracture fatigue and wear (FFW 2021) (Lecture notes in mechanical engineering), Springer, Ghent, Belgium
22. Kant C, Harmain GA (2021) Analysis of single overload effect on fatigue crack propagation using modified virtual crack annealing model. In: International conference on mechanical engineering
23. Kant C, Harmain GA (2021d) A model based study of fatigue life prediction for multifarious loadings. Key Eng Mater 882:296–327. https://www.scientific.net/KEM.882.296
24. Kanth SA, Harmain GA, Jameel A (2021) Investigation of fatigue crack growth in engineering components containing different types of material irregularities by XFEM. Mech Adv Mater Struct1–39. https://doi.org/10.1080/15376494.2021.1907003
25. Kanth SA, Harmain GA, Jameel A (2018) Modeling of nonlinear crack growth in steel and aluminum alloys by the element free Galerkin method. Mater Today Proc 5(9):18805–18814
26. Kanth SA, Lone AS, Harmain GA, Jameel A (2019) Elasto plastic crack growth by XFEM: a review. Mater Today Proc 18:3472–3481. https://doi.org/10.1016/j.matpr.2019.07.275
27. Kanth SA, Lone AS, Harmain GA, Jameel A (2019b) Modeling of embedded and edge cracks in steel alloys by XFEM. Mater Today Proc 26(xxxx):814–18. https://doi.org/10.1016/j.matpr.2019.12.423
28. Kim DW, Chang J-H, Ryu W-S (2008) Evaluation of the creep-fatigue damage mechanism of type 316L and type 316LN stainless steel. Int J Press Vessels Pip 85(6):378–384
29. Kim DW, Kim WG, Ryu W-S (2003) Role of dynamic strain aging on low cycle fatigue and crack propagation of type 316L (N) stainless steel. Int J Fatigue 25(9–11):1203–1207
30. Krishnan SA et al (2015) Coupled FEM and experimental analysis to characterize initial crack growth regime in AISI 316L (N) stainless steel. Int J Struct Integrity 6:390–401
31. Kumar JG et al (2010) High temperature design curves for high nitrogen grades of 316LN stainless steel. Nucl Eng Des 240(6):1363–1370
32. Li B et al (2020) Cyclic deformation and cracking behavior of 316LN stainless steel under thermomechanical and isothermal fatigue loadings. Mater Sci Eng A 773:138866
33. Li B et al. (2021) Cyclic deformation behavior and dynamic strain aging of 316LN stainless steel under low cycle fatigue loadings at 550 °C. Mater Sci Eng A 818(November 2020):141411. https://doi.org/10.1016/j.msea.2021.141411
34. Lone AS, Jameel A, Harmain GA (2018) A coupled finite element-element free Galerkin approach for modeling frictional contact in engineering components. Mater Today Proc 5(9):18745–18754. https://doi.org/10.1016/j.matpr.2018.06.221
35. Lone AS, Kanth SA, Harmain GA, Jameel A (2019) XFEM Modeling of frictional contact between elliptical inclusions and solid bodies. Mater Today Proc 26(xxxx): 819–24. https://doi.org/10.1016/j.matpr.2019.12.424

36. Lone AS, Kanth SA, Jameel A, Harmain GA (2019) A state of art review on the modeling of contact type nonlinearities by extended finite element method. Mater Today Proc 18:3462–3471. https://doi.org/10.1016/j.matpr.2019.07.274
37. Mathew MD, Laha K, Sandhya R (2013) Creep and low cycle fatigue behaviour of fast reactor structural materials. Proc Eng 55:17–26
38. Mathew MD, Sasikala G, Bhanu Sankara Rao K, Mannan SL (1991) Influence of carbon and nitrogen on the creep properties of type 316 stainless steel at 873 K. Mater Sci Eng A 148(2):253–260
39. Nam SW et al (1996) The normalized coffin-manson plot in terms of a new damage function based on grain boundary cavitation under creep-fatigue condition. Metall Mater Trans A 27(5):1273–1281
40. Nilsson JO (1988) Effect of nitrogen on creep-fatigue interaction in austenitic stainless steels at 600 °C. In: Low cycle fatigue, ASTM International
41. Oh YJ, Ryu WS, Hong JH (1997) The effect of nitrogen on the grain boundary precipitation and sensitization of Type 316 L stainless steels. J Korean Inst Met Mater (South Korea) 35(8):942–50
42. Palaparti DP, Rao V, Ganesan JC, Prasad Reddy GV (2021) Tensile flow analysis of austenitic type 316LN stainless steel: effect of nitrogen content. J Mater Eng Perform 30(3):2074–2082. https://doi.org/10.1007/s11665-021-05484-y
43. Reddy GV, Prasad RK et al (2015) Effect of strain rate on low cycle fatigue of 316LN stainless steel with varying nitrogen content: part-I cyclic deformation behavior. Int J Fatigue 81:299–308
44. Reddy GV, Prasad AN et al (2015) Thermomechanical and isothermal fatigue behavior of 316LN stainless steel with varying nitrogen content. Metall Mater Trans A 46(2):695–707
45. Reddy GV, Prasad RS, Bhanu Sankara Rao K, Sankaran S (2010) Influence of nitrogen alloying on dynamic strain ageing regimes in low cycle fatigue of AISI 316LN stainless steel. Proc Eng 2(1):2181–2188
46. Reddy GV, Prasad RS, Sankaran S, Mathew MD (2014) Low cycle fatigue behavior of 316LN stainless steel alloyed with varying nitrogen content part I: cyclic deformation behavior. Metall and Mater Trans A 45(11):5044–5056
47. Reddy GV, Prasad RS, Sankaran S, Mathew MD (2014) Low cycle fatigue behavior of 316LN stainless steel alloyed with varying nitrogen content part II: fatigue life and fracture behavior. Metall Mater Trans A 45(11):5057–5067
48. Rodriguez P, Bhanu Sankara K, Rao. (1993) Nucleation and growth of cracks and cavities under creep-fatigue interaction. Prog Mater Sci 37(5):403–480
49. Roy SC, Sunil Goyal R, Sandhya, and S K Ray. (2013) Analysis of hysteresis loops of 316L (N) stainless steel under low cycle fatigue loading conditions. Proc Eng 55:165–170
50. Samantaray D et al (2017) Plastic deformation of SS 316LN: thermo-mechanical and microstructural aspects. Proc Eng 207:1785–1790
51. Samantaray D, Mandal S, Phaniraj C, Bhaduri AK (2011) Flow behavior and microstructural evolution during hot deformation of AISI type 316 L (N) austenitic stainless steel. Mater Sci Eng A 528(29–30):8565–8572
52. Samuel EI, Choudhary BK, Bhanu Sankara K, Rao (2002) Influence of temperature and strain rate on tensile work hardening behaviour of Type 316 LN austenitic stainless steel. Scripta Mater 46(7):507–512
53. Samuel KG, Sasikala G, Ray SK (2011) On R ratio dependence of threshold stress intensity factor range for fatigue crack growth in type 316(N) stainless steel weld. Mater Sci Technol 27(1):371–376
54. Samuel KG, Mannan SL, Rodriguez P (1988) Serrated yielding in AISI 316 stainless steel. Acta Metall 36(8):2323–2327
55. Sarkar A, Nagesha A, Parameswaran P et al (2013) Influence of dynamic strain aging on the deformation behavior during ratcheting of a 316LN stainless steel. Mater Sci Eng A 564:359–368
56. Sarkar A et al (2018) Manifestations of dynamic strain aging under low and high cycle fatigue in a type 316LN stainless steel. Mater High Temp 35(6):523–528

57. Sarkar A, Dash MK, Nagesha A (2021) Mechanism of HCF-creep interaction in a Type 316LN stainless steel. Mater Sci Eng A 825(July):141841. https://doi.org/10.1016/j.msea.2021.141841
58. Sarkar A, Nagesha A, Sandhya R, Mathew MD (2013) Effect of Temperature on ratcheting behaviour of 316LN SS. Proc Eng 55:650–654
59. Sarkar A, Nagesha A, Sandhya R, Mathew MD (2015) A perspective on fatigue damage by decoupling LCF and HCF loads in a type 316LN stainless steel. High Temp Mater Process (London) 34(5):435–439
60. Sasikala G, Babu MN, Dutt BS, Venugopal S (2013) Characterisation of fatigue crack growth and fracture behaviour of SS 316L (N) base and weld materials. Trans Tech Publ, In Advanced Materials Research, pp 449–459
61. Sauzay M et al (2004) Creep-fatigue behaviour of an AISI stainless steel at 550 °C. Nucl Eng Des 232(3):219–236
62. Schwartz J, Fandeur O, Rey C (2010) Modelling of Low Cycle Fatigue Initiation of 316LN Based on crystalline plasticity and geometrically necessary dislocations. Trans Tech Publ, In Materials Science Forum, pp 1137–1142
63. Sistaninia M, Niffenegger M (2015) Fatigue crack initiation and crystallographic growth in 316L stainless steel. Int J Fatigue 70:163–170
64. Srinivasan VS et al (1991) Effects of temperature on the low cycle fatigue behaviour of nitrogen alloyed type 316L stainless steel. Int J Fatigue 13(6):471–478
65. Srinivasan VS et al (1999) High temperature time-dependent low cycle fatigue behaviour of a type 316L (N) stainless steel. Int J Fatigue 21(1):11–21
66. Srinivasan VS et al (2003) Low cycle fatigue and creep-fatigue interaction behavior of 316L (N) stainless steel and life prediction by artificial neural network approach. Int J Fatigue 25(12):1327–1338
67. Suresh Kumar T, Nagesha A, Mariappan K, Dash MK (2021) Deformation and failure behaviour of 316 LN austenitic stainless steel weld joint under thermomechanical low cycle fatigue in as-welded and thermally aged conditions. Int J Fatigue 149(January):106269. https://doi.org/10.1016/j.ijfatigue.2021.106269
68. Taylor D, Knott JF (1981) Fatigue crack propagation behaviour of short cracks; the effect of microstructure. Fatigue Fract Eng Mater Struct 4(2):147–155
69. Valsan M, Nagesha A (2010) Low cycle fatigue and creep-fatigue interaction behaviour of 316L(N) stainless steel and its welds. Trans Indian Inst Met 63(2–3):209–215
70. Vogt JB et al (1991) Low-temperature fatigue of 316L and 316LN austenitic stainless steels. Metall Trans A 22(10):2385–2392
71. Wang S, Zhang M, Wu H, Yang B (2016) Study on the dynamic recrystallization model and mechanism of nuclear grade 316LN austenitic stainless steel. Mater Charact 118:92–101
72. Wang S, Yang K, Shan Y, Li L (2008) Plastic deformation and fracture behaviors of nitrogen-alloyed austenitic stainless steels. Mater Sci Eng A 490(1–2):95–104
73. Yan X-l, Zhang X-C, Shan-tung T, Mannan S-L (2015) International journal of pressure vessels and piping review of creep e fatigue endurance and life prediction of 316 stainless steels. Int J Press Vessels Pip 126–127:17–28
74. Zhang X, Shan-Tung T, Xuan F (2014) Creep–fatigue endurance of 304 stainless steels. Theoret Appl Fract Mech 71:51–66
75. Zhang X, Zhang Y, Li Y, Liu J (2013) Cracking initiation mechanism of 316LN stainless steel in the process of the hot deformation. Mater Sci Eng, A 559:301–306
76. Zheng Y et al. (2022) Multiaxial low cycle fatigue behavior and life prediction method of 316LN stainless steel at 550 °C. Int J Fatigue 156(October 2021): 106637. https://doi.org/10.1016/j.ijfatigue.2021.106637